Author Manuscript

Author Manuscript

Author Manuscript

Author Manuscript

HHS Public Access

Author manuscript

Int J Radiat Oncol Biol Phys. Author manuscript; available in PMC 2018 October 01.

Published in final edited form as:

Int J Radiat Oncol Biol Phys. 2017 October 01; 99(2): 325–333. doi:10.1016/j.ijrobp.2017.04.024.

Evaluating the toxicity reduction with CT-ventilation functional avoidance radiotherapy

Austin M. Faught[1,*], **Yuya Miyasaka**[2], **Noriyuki Kadoya**[2], **Richard Castillo**[3], **Edward Castillo**[4], **Yevgeniy Vinogradskiy**[1], and **Tokihiro Yamamoto**[5]

[1]University of Colorado School of Medicine, Aurora, Colorado

[2]Tohoku University Graduate School of Medicine, Sendai, Miyagi

[3]University of Texas Medical Branch of Galveston, League City, Texas

[4]Beaumont Health System, Royal Oak, Michigan

[5]UC Davis School of Medicine, Sacramento, CA

Summary

A retrospective study of 70 lung cancer patients with 4DCT images was performed to estimate the toxicity reduction achieved when using CT-ventilation functional avoidance radiotherapy in place of traditional radiotherapy. Normal tissue complication probability (NTCP) models were developed from clinically used plans based on dose to functional lung. Thirty patients were re-planned using functional avoidance techniques and RTOG 0617 constraints, and the reduction in lung toxicity was assessed using the NTCP models.

Purpose—CT-ventilation imaging is a new modality that uses 4DCT information to calculate lung ventilation. While retrospective studies have reported on the reduction in dose to functional lung, no work has been published in which the dosimetric improvements have been translated to a reduction in the probability of pulmonary toxicity. Our work estimates the reduction in toxicity for CT-ventilation based functional avoidance planning.

Methods and Materials—Seventy previously treated lung cancer patients with 4DCT imaging were used for the study. CT-ventilation maps were calculated using the 4DCT, deformable image registration, and a density-change-based algorithm. Pneumonitis was graded based on imaging and clinical presentation. Maximum-likelihood methods were used to generate normal tissue complication probability (NTCP) models predicting grade 2 or higher (2+) and grade 3+ pneumonitis as a function of dose (V5Gy, V10Gy, V20Gy, V30Gy, and mean dose) to functional lung. For thirty patients a functional plan was generated with the goal of reducing dose to the functional lung while meeting RTOG 0617 constraints. The NTCP models were applied to the functional plans and the clinically-used plans to calculate toxicity reduction.

[*]Corresponding Author: University of Colorado School of Medicine, 1665 Aurora Ct. Suite 1032, Campus Mail Stop R-706, Denver, CO 80045, Tel: (720) 848-0133, Fax: (720) 848-0481, austin.faught@ucdenver.edu.

Conflict of Interest: This work was partially funded by grant R01CA200817 (AF, RC, EC, YV) and 1K01-CA-181292-01 (RC)

Publisher's Disclaimer: This is a PDF file of an unedited manuscript that has been accepted for publication. As a service to our customers we are providing this early version of the manuscript. The manuscript will undergo copyediting, typesetting, and review of the resulting proof before it is published in its final citable form. Please note that during the production process errors may be discovered which could affect the content, and all legal disclaimers that apply to the journal pertain.

Author Manuscript Author Manuscript Author Manuscript Author Manuscript

Results—Using functional avoidance planning, absolute reductions in grade 2+ NTCP of 6.3%, 7.8% and 4.8% were achieved based on the mean fV20Gy, fV30Gy, and fMLD metrics, respectively. Absolute grade 3+ NTCP reductions of 3.6%, 4.8%, and 2.4% were achieved with fV20Gy, fV30Gy, and fMLD. Maximum absolute reductions of 52.3% and 16.4% were seen for grade 2+ and grade 3+ pneumonitis for individual patients.

Conclusion—Our study quantifies the possible toxicity reduction from CT-ventilation-based functional avoidance planning. Reductions in grades 2+ and 3+ pneumonitis were 7.1% and 4.7% based on mean dose-function metrics with reductions as high as 52.3% for individual patients. Our work provides seminal data for determining the potential toxicity benefit from incorporating CT-ventilation into thoracic treatment planning.

Introduction

Lung cancer, with an estimated 224,390 new cases and 158,080 deaths in 2016, is the second most common form of cancer among both sexes and the leading cause of cancer death in the United States (1). The challenge in treating lung cancer is that the disease is aggressive, there are numerous nearby organs at risk such as the esophagus, trachea, heart, brachial plexus, and spinal cord, and the surrounding healthy lung tissue is both radiosensitive and critical to patient survival. As a result, the limiting factor in planning a course of treatment is the normal tissue tolerance to radiation(2-5).

Advances in radiotherapy technology such as stereotactic body radiation therapy (SBRT) have allowed for increasingly conformal doses to the target volume. Improved conformality has facilitated dose escalation studies that aim to increase target dose while maintaining the normal tissue tolerances established in previous studies(6-8). Established normal tissue tolerance limits derive from the simplifying assumption of homogeneous underlying lung function. However, functional heterogeneity has been demonstrated in a large portion of stage III cases(9,10). Different functional imaging modalities of lung ventilation such as single photon emission computed tomography (SPECT), hyperpolarized Helium or Xenon MRI, breath-hold CT ventilation, and more recently 4DCT ventilation imaging have sought to identify areas of high functioning lung (11-16). The physiological information from these modalities can be used to assess treatment response or to create a treatment plan that preferentially spares areas of high functioning lung.

4DCT ventilation is an imaging modality that uses phase resolved CT images to calculate pulmonary ventilation(17-21). Because the acquisition of a 4DCT is increasingly common amongst lung cancer patients, 4DCT ventilation images can be calculated at no extra financial or dosimetric cost to the patient. Recent studies published in the literature report on the methodology of 4DCT ventilation imaging(19,21), its validation(19,21-28), and different clinical uses for it as a functional imaging modality(12,29-32).

The ability to map areas of high functioning lung using CT-ventilation imaging allows for preferential sparing of the functioning lung in the treatment planning process with the goal of reducing pulmonary toxicity. Many of the current studies in the literature have demonstrated dosimetric reductions that are achievable using this form of planning (2,14,15), nominally referred to as functional avoidance planning, but there are no studies

Author Manuscript Author Manuscript Author Manuscript Author Manuscript

that have attempted to quantify the impact of functional avoidance planning on toxicity reductions. The work presented in this paper estimates the reduction in radiation pneumonitis based on a retrospective analysis of 70 lung cancer patients presenting with heterogeneous lung function as assessed from CT-ventilation images.

Methods

Patient Population

Patients were retrospectively selected from a previously reported cohort (21) consisting of non-small-cell lung cancer patients who had received 4DCTs and radiation pneumonitis toxicity grading. Of the 96 available patients, 70 were selected for the current study based on functional heterogeneity criteria previously presented (10) and used for our ongoing clinical trial (NCT02528942). This method of calculation divides each lung into three superior-to-inferior sections. The average ventilation in each of the six sections is added together and divided by six to get what one would expect to be the ventilation value throughout the lung if function was perfectly homogeneous. We defined anything deviating by more than 15% lower than that homogeneous value as non-functioning. The heterogeneity criterion is imposed to ensure that there are functional regions to preferentially spare. If a patient's ventilation image is heterogeneous and displays a major ventilation defect, functional avoidance can preferentially deposit dose in the defect area as opposed to the functional area.

Among the 70 patients used for this study, 8 were Stage 1, 9 were Stage 2, 49 were Stage 3, and 4 were Stage 4. Forty-one of the selected patients received IMRT (58.6%) for treatment and 29 (41.4%) received 3D conformal radiation therapy. All patients were treated with standard fractionation schemes (1.8Gy-2.0Gy per fraction).

The clinical endpoints for analysis were grade 2 or higher (denoted as grade 2+) and grade 3+ radiation pneumonitis, both of which were determined retrospectively using the patients' clinical charts and radiographic findings. Scoring was done using the Common Terminology Criteria for Adverse Events (version 3.0) scoring system which defines grade 3 pneumonitis as symptomatic, interfering with daily activities, or O_2 indicated, and grade 2 pneumonitis as symptomatic and not interfering with daily activities. Of the seventy selected patients, 26/70 (37%) were scored as grade 2+ and 14/70 (20%) were scored as grade 3+.

Ventilation Image Calculation

The ventilation images were calculated from pre-treatment 4DCTs for each patient. The lungs were segmented to exclude the trachea, main-stem bronchi, pulmonary vasculature, and the gross tumor volume for both the inhale and exhale images (21). Deformable image registration was used to link voxels in the peak-inhale phase with those in the peak-exhale phase. The deformation algorithm was reported to have a spatial accuracy of 1.25mm in a previous study (33). After segmentation and registration, the Hounsfield units were used in a density change-based model given in Equation 1.

Author Manuscript Author Manuscript Author Manuscript Author Manuscript

$$\frac{V_{\text{in}} - V_{\text{ex}}}{V_{\text{ex}}} - 1000\frac{HU_{\text{in}} - HU_{\text{ex}}}{HU_{\text{ex}}(1000+HU_{\text{in}})} \quad (1)$$

In the equation, V_{in} and V_{ex} are the inhale and exhale volumes, respectively, and HU_{in} and HU_{ex} are the Hounsfield units of the individual lung voxels from the inhale and exhale phases, respectively. The density change-based formalism assumes a linear combination of water-like material with HU value of 0 and air-like material with HU value of-1000 (34). The calculation is performed for each voxel within the lung to form a 3D map of the ventilation. (2,21). The ventilation images and deformation maps are manually inspected to ensure there are no major artifacts or discontinuities present.

Toxicity Modeling

Using the 70 patient cohort, normal tissue complication probability (NTCP) models were fit using maximum-likelihood methods for the fractional volume of functional lung receiving 5Gy, lOGy, 20Gy, and 30Gy (fV5Gy, fVlOGy, fV20Gy, and fV30Gy, respectively) as well as the mean dose to functional lung (fMLD). All doses used in modeling were physical doses recorded by the treatment planning system. The models were used to generate receiver operating characteristic (ROC) curves in which the area under the curve (AUC) could be used to assess the predictive power of the models. The model fitting parameters, logistic regression significance (p) results, and AUC values are presented for each model. To establish 95% confidence intervals on the NTCP values of generated models, bootstrap analysis was performed with 2000 bootstrap samples(35).

Functional Planning

Thirty of the seventy patients were selected for functional planning evaluation. The 30 patient subset was verified to have similar toxicity and dosimetric characteristics to the 70 patient population as determined by incidence of pneumonitis and mean lung dose. For the 30 patients selected for functional avoidance planning, a structure was created in the Eclipse treatment planning system (Varian Medical Systems, Palo Alto, CA) corresponding to functional lung. The binary functional lung structure was generated by application of a predetermined defect threshold to the CT-ventilation image. Areas of ventilation defect were defined as regions with a greater than 15% reduction from a perfectly homogenous lung function (see Appendix A for full explanation). Regions of lung above the 15% threshold were considered areas of high-function and included in the functional contour used in planning.

Using the IMRT optimizer in the Eclipse treatment planning system, dose to the functional structure was minimized while also attempting to honor RTOG 0617-based constraints used for normal clinical planning. In general, when an optimizer is pushed to reduce dose to functional lung, other dosimetric parameters are sacrificed. Priority was given to the RTOG 0617 constraints to ensure a clinically acceptable plan. Beam placement for functional plans was left up to the planner and chosen in order to minimize the amount of functional lung traversed while meeting all other target and OAR constraints. All plans ensured that 95% of

Author Manuscript Author Manuscript Author Manuscript Author Manuscript

the planning target volume was receiving the prescription dose. Dose calculations were performed using the Analytical Anisotropic Algorithm (AAA).

Toxicity Reduction Calculations

Using the generated NTCP models, the probabilities of grade 2+ and grade 3+ pneumonitis were calculated for the clinical plans (plan used to treat the patient) and functional plans of the thirty patient planning cohort. The toxicity probability for the average patient was calculated by using the average dose metric (e.g. V20Gy) from the 30 patient cohort and the associated NTCP model generated from the full 70 patient modeling cohort. Due to the non-linear nature of the probit model, this is not the same as averaging the individual toxicity reductions of the 30 patient cohort. The former method, and method of choice, can be thought of as an estimate of the toxicity reduction to an average patient while the latter method is a toxicity estimate to the candidate population. Absolute and relative changes in probabilities of complications were compared between functional avoidance plans and the clinically used plans to determine the extent to which toxicity probabilities were reduced due to functional avoidance planning. During the bootstrap analysis toxicity reductions were calculate for each of the 2000 bootstrap samples in order to establish 95% confidence intervals on the toxicity reductions.

Results

Table 1 presents the modeling results predicting the probability of radiation pneumonitis as a function of functional-dose metrics. Along with a complete list of AUC and p-values, Table 1 also presents the generated fitting parameters, the inverse of the slope of the curve, m, and the 50% complication probability dose, TD_{50}, for both grade 2+ and grade 3+ prediction models. The volume of functional lung receiving ≥10Gy (fV10Gy) and the mean dose to functional lung were the best predictors for grade 2+ toxicities. The models for the two metrics had an AUC of 0.718 and p-value <0.01 and an AUC of 0.723 and p-value <0.01, respectively

The quality of the models generated for predicting grade 3+ toxicities was comparatively worse for volumes of functional lung receiving lower doses (fV5Gy and fV10Gy). This is reflected in the AUC values and non-significance in fit as established by the reported p-Values. Models with the highest predictive power were for volumes of functional lung receiving ≥20Gy and ≥30Gy (p = 0.011, AUC = 0.674 and p=0.013, AUC = 0.671, respectively).

Figure 1 shows a representative example comparing a functional plan (right) with the clinically used plan (left). Shown in the figure are a CT ventilation image (with brighter colors corresponding to areas of the lung with increased pulmonary ventilation), the PTV, and overlaid isodose lines corresponding to 5Gy, 10Gy, 20Gy, 30Gy, and 70Gy. Observable reductions in dose to the high functioning area in the posterolateral right lung are present in the example. An illustration of how the reduction in toxicity was calculated is shown in Figure 2. Figure 2 shows the dose-response model predicting grade 2+ pneumonitis as a function of fV30Gy. Transposed on the model is the average fV30 values for the clinical and functional plans and the corresponding toxicity estimates. For the dose-response curve

Author Manuscript Author Manuscript Author Manuscript Author Manuscript

generated in Figure 2, a reduction in fV30Gy from 24.3% to 19.9% results in change in probability of developing grade 2+ radiation pneumonitis of 38.3% to 30.5%, an absolute reduction of 7.8%.

Toxicity probabilities based on functional dose metrics were calculated for each of the 30 patients that were re-planned using functional avoidance techniques. The calculated toxicity probability for each plan, using each functional dose metric, was calculated and compared to the clinically used plan. The average value of the dose metrics used is reported for clinical plans and functional avoidance plans in Table 2. The clinical toxicity probability of the mean metric and associated reduction in toxicity is presented in Table 3 for grade 2+ toxicities for all functional dose metrics. Absolute reductions in grade 2+ toxicity were as high as 8.0% (based upon fV10Gy) and as small as 4.4% (based on fV5Gy). Estimated grade 3+ toxicity reductions, presented in Table 4, were as high as 4.8% for fV30Gy and as low as 2.4% for fMLD. Estimated reductions of grade 3+ toxicities based off of fV5Gy and fV10Gy were not included because the models did not demonstrate statistical significance. Toxicity reductions presented in Tables 3 and 4 are calculated from the mean dose metric (e.g. average fV20Gy among the 30 patient sub-sample) applied to the NTCP models. Individual patients showed absolute probability reductions as high as 52.3% and 16.4% for grade 2+ and grade 3+ toxicities, respectively. The ranges of toxicity reduction presented in Tables 3 and 4 demonstrate instances of a negative change, which corresponds to an increased probability of toxicity with functional planning compared to the clinical plans. Also presented in Tables 3 and 4 are the calculated 95% confidence intervals for the NTCP values and toxicity reductions as determined from the bootstrapping analysis.

Discussion

Results from the NTCP models showed strong predictive capacity for grade 2+ and 3+ pneumonitis when evaluating dose metrics to functional lung volumes. The metrics with greatest predictive power with respect to grade 3+ toxicities were fV30Gy and fV20Gy (AUC of 0.671 and 0.674, respectively). For grade 2+ toxicities all metrics had AUC values greater than 0.682 (fV30Gy), with the greatest predictive power being associated with fV10Gy and fMLD (0.718 and 0.723, respectively). The volume of functional lung receiving low doses (e.g. 5Gy) had the poorest performance of presented models. This was especially true when examining low dose to the entire lung (non-functional metrics). The poor model performance is reflected in poor p-Values of the models, non-intuitive model parameters (i.e. TD_{50} and m) that indicated the models did not converge to a solution, and the large range in the reported 95% confidence intervals. In other words we did not observe a dose response at the low dose level. Inclusion of the results for the low dose models was done for completeness and comparison to the more predictive higher dose models. Clinical significance should not be assigned to the poorer performing models.

The predictive power of our NTCP models based on functional metrics compares favorably to previously reported models in the literature. Lind et al published NTCP models for grade 2+ pneumonitis with AUCs up to 0.68 for uni-dimensional modeling and 0.72 for bi-dimensional models(36). Vinogradskiy et al published results of grade 2+ modeling for both dose-volume and dose-function metrics with AUCs up to 0.544 and 0.620, respectively(29).

Author Manuscript Author Manuscript Author Manuscript Author Manuscript

In addition to pneumonitis, functional volume based models predicting radiation fibrosis have been published(37) with AUC values as high as 0.85. Our values for grade 2+ models (AUC >0.7 for fV10Gy, fV20Gy, and fMLD) exceed the uni-dimensional models for radiation pneumonitis and are in in-line with the bi-dimensional models of the published results. These prior studies and our results all support the concept of functional avoidance planning.

By reducing dose to areas of functional lung during functional avoidance planning, the probability of normal tissue complications was measurably reduced. The greatest effect was observed when applying models based on the volume of functional lung receiving ≥30Gy. For these models, probabilities were reduced on average by 7.1% and 4.7% for grade 2+ and grade 3+ toxicities, respectively. Overall, our results revealed that typical reductions of 6% and 3% can be expected for grade 2+ and 3+ radiation pneumonitis respectively with functional planning. The absolute toxicity rate in our patient cohort was 37% for grade 2+ radiation pneumonitis and 20% for grade 3+ radiation pneumonitis. Based on our data, the rate of toxicity can be reduced to 31% (relative reduction of 16%) for grade 2+ pneumonitis and 15% (relative reduction of 25%) for grade 3+ pneumonitis with functional planning. The relative reductions of 16% and 25% make our results applicable to other data sets whose actual toxicity incidence rates differ from our data sets. As a part of our analysis we calculated 95% confidence intervals on both the NTCP values and the toxicity reductions. While the confidence intervals on the NTCP values were large (as high as a 26% window), the confidence intervals on the actual toxicity reduction demonstrate a consistent relationship between the toxicities of the clinical and functional plans that support a reduction in toxicity when utilizing functional avoidance planning. In other words, the relationship between toxicity probability of the clinical plans and functional plans was consistently in favor of the functional plan throughout bootstrap analysis.

We also noted that for individual patients, absolute reductions in toxicity as high as 52% (grade 2+) and 16% (grade 3+) were achieved with functional planning. The ranges in Tables 3 and 4 also show instances of negative values, which correspond to a higher probability of toxicity with functional plans compared to the clinical plans. The wide range of changes in toxicity probability speaks to the dependence on patient-specific distributions of functionality with respect to tumor location. In individual plans certain dose metrics to functional lung can be increased while others are reduced, resulting in an estimated increase in toxicity probability. Results from future clinical trials will need to be used to determine which dose metrics are most critical in assessing a treatment plan.

Functional avoidance planning has been previously explored using SPECT(38-40), PET/CT(41), and CT-ventilation imaging(2,13). The average functional volume receiving ≥20Gy (fV20Gy) and mean dose to functional lung (fMLD), 26.8% and 17.8Gy, respectively, were comparable to a previous study (33.8% and 18.3Gy)(42) investigating the potential dosimetric savings of functional avoidance planning using CT-ventilation imaging. A previous study by Kida et al. (42) compared functional avoidance planning based on SPECT ventilation images to that based on 4DCT ventilation imaging. The two forms of functional avoidance planning showed strong correlation (R=0.94) between reductions to functional lung and the maximum observed difference in fV20 was just 2.8%. The correlation results of

Author Manuscript Author Manuscript Author Manuscript Author Manuscript

the Kida study as well as the consistent dosimetry results with the previously mentioned studies assured that the results in toxicity reduction were not specific to this study, but achievable in other functional avoidance planning studies.

Functional avoidance planning has been increasingly explored in the literature, but to date only dosimetric demonstrations in the reduction of functional lung dose have been published. The results of this study are the first to translate the reduction in dose to functional lung (as measured by CT-ventilation) to a reduction in the risk of radiation toxicities to lung cancer patients. There remains uncertainty in which combination of functional dose metric and cutoff between functional and non-functional lung should be used in the optimization process. Ultimately, the ideal means of optimization will be determined by clinical trials. There are numerous clinical trials underway aimed at prospectively assessing functional avoidance planning (NCT02528942, NCT02773238, NCT02002052, NCT02308709, NCT01034514, NCT02843568); the data presented in the current study can prove vital in estimating the anticipated results of potential toxicity reduction with functional avoidance.

There were several limitations to our study. About half of the patients had been treated by 3D conformal techniques as opposed to IMRT. Among the patients treated with IMRT, an older version of the optimizer was used in the planning process owing to the data set extending back up to ten years. It is also important to recognize that the estimated toxicity reductions were for patients with heterogeneous lung function only. Theoretically, patients with heterogeneous lung function stand to benefit most from functional avoidance planning, and the estimated reductions should not be interpreted as applicable to the entire lung cancer population. Based on a previous study (10), about 65% of stage iii lung cancer patients can be expected to display heterogeneous lung function.

While there were functional plans that violated RTOG 0617 constraints, in all those cases the plan had been challenging (typically a large treatment volume) and the constraint had been violated in the original clinical plan (and deemed clinically acceptable by the radiation oncologist). The most commonly violated normal tissue constraints were mean esophagus dose ≤34Gy (12/30 and 16/30 violated for functional and standard plans, respectively) and lung V20Gy ≤37% (6/30 and 9/30 violated for functional and standard plans, respectively). A summary of the normal tissue constraints in RTOG 0617 is presented in Appendix B along with average dose values for each metric from both clinical and functional avoidance plans. The minimum dose to the PTV was consistently less than 95% of the prescription dose for functional and clinical plans. It is important to stress that dose to functional lung should not be reduced at the expense of violating already established normal tissue tolerances. As an additional means of demonstrating that the reductions in dose to functional lung did not come at the expense of normal lung dose metrics, NTCP models and toxicity reductions were calculated based off of both a dose to functional lung metric and a corresponding dose to total lung metric and are presented in Appendix C. The comparable estimates in toxicity reduction in the two variable models and adherence to clinically relevant planning criteria (RTOG 0617) justified the use of single parameter modeling in this study.

Author Manuscript Author Manuscript Author Manuscript Author Manuscript

CT-ventilation imaging is a new technology which is continually being improved. Efforts are being made to address imaging artifacts, deformable image registration uncertainties(43), normalization techniques(44), and the means of calculating ventilation(28). Work is still being done to comprehensively validate 4DCT-ventilation and evaluate the reproducibility. Castillo et al. have shown favorable regional comparisons between density change based 4DCT ventilation and ^{99m}Tc-labeled aerosol SPECT/CT ventilation imaging(21). Significant, albeit moderate, correlations were found with respect to pulmonary function tests (PFT) (absolute value of Pearson correlation coefficients of 0.63 to 0.73) and ^{99m}Tc-labeled aerosol SPECT/CT ventilation imaging (Dice similarity coefficients of 0.35 to 0.46) in a study by Yamamoto et al.(23). Kipriditis et al. validated the density change-based CT ventilation imaging against ^{68}Ga-labeled nanoparticles for positron emission tomography (PET) and demonstrated correlation coefficients ranging from 0.22 to 0.76 (28). While the studies have all shown promising results for 4DCT ventilation imaging as a means of imaging regional air volume change, continued work on its validation against other lung functional imaging (e.g. SPECT, PET, MRI, etc.) and measures of lung function (e.g. PFT) are warranted in larger populations.

The dose and function metrics presented in this work and used for calculating toxicity probabilities assume a static relationship between the location of the dose and the spatial distribution of high functionality. Previous studies have shown that as the tumor shrinks in response to therapy areas of previous ventilation defects can be reventilated due to reopening of airways(45). Radiation pneumonitis was used as the clinical end-point in assessing patient toxicities for this study due to its clinical significance. There are other potential toxicities in radiation therapy for lung cancer that have been studied for functional avoidance therapy(37). The authors felt that in spite of the limitations of the dataset and methods, this work was valuable in providing an estimate on the effect of functional avoidance planning.

Conclusion

CT-ventilation imaging is an exciting new imaging modality that allows for the calculation of pulmonary ventilation from 4DCT scans. With most lung cancer patients receiving 4DCT scans as a part of the standard of care, CT-ventilation allows for assessment of lung function without any additional burden to the patient. In using the ventilation maps to create treatment plans that preferentially avoid higher functioning areas of the lung, the rate of pulmonary toxicity can theoretically be reduced. In this study we have shown that reductions in grades 2+ and 3+ radiation pneumonitis based off of mean dose-function metrics can be as high as 8.0% and 4.8%, respectively, with individual patient reductions as high as 52.3%. Our work provides the first estimates of the potential reduction in pulmonary complications with CT-ventilation based functional avoidance.

Supplementary Material

Refer to Web version on PubMed Central for supplementary material.

Author Manuscript Author Manuscript Author Manuscript Author Manuscript

Appendix A

Areas of ventilation defect were identified by calculating the percent deviation from a perfectly homogeneous lung function map. The calculation utilized a technique employed in nuclear medicine which divides the lung into superior-inferior thirds to assess lung function heterogeneity. The division of lung function into geometric thirds has been employed in the assessment of CT-ventilation imaging (10). The calculation assumes that in a healthy set of lungs with homogenous function, each third would constitute 16.7% (100% divided evenly by 6) of the total ventilation measured from the CT-ventilation map. Areas of ventilation defect were identified as regions in which the ventilation values were below a set threshold (15% deviation for this study) from the expected average in a homogenous lung. Mathematically the calculation of the cutoff ventilation value, V_C, is illustrated in Equation 2.

$$V_T = \left(\frac{100}{6}\right)\left(\frac{100-x}{100}\right)\sum_{i=1}^{6} V_{\mathrm{ave},i} \quad (2)$$

Where x is the percent reduction from homogeneous function, 15% in our study, and $V_{ave,i}$ is the average ventilation value of the Ah third. All voxels with ventilation values greater than V_T were classified as functional lung and included in the functional lung contour used to calculate functional dose metrics and optimize the functional avoidance plans.

The 15% reduction from homogenous lung function was based on metrics derived from our previous work (10) and showed the best correlation with user-identified defects (46). There have been several proposals on how to best define ‘functional’ lung (37,47,48). The 15% threshold and the above-described approach were chosen based on previous image heterogeneity analysis (10), the correlation of image heterogeneity metrics with radiologist interpretations (46), and our clinical trial imaging criteria workflow (NCT02528942). Final methods for determining a ‘functional’ contour from the ventilation image will be based on clinical toxicity results from the on-going clinical trials; however, in the absence of quantitative guidelines for assessing ventilation heterogeneity, we believe the method presented provides a logical starting point.

Appendix B

Table 1

A summary of the RTOG 0617 constraints used in planning are presented with the average values of the clinical plans used for NTCP modeling and the average values in the functional plans after functional avoidance planning.

Organ	Constraint	Clinical Plan Average	Functional Plan Average
Spinal Cord	Max Dose < 50.5Gy	44.15Gy	47.58Gy
Lung	V20Gy < 37%	32.55%	31.57%
	Mean Dose < 20Gy	20.63Gy	20.55Gy

Author Manuscript Author Manuscript Author Manuscript Author Manuscript

Organ	Constraint	Clinical Plan Average	Functional Plan Average
Esophagus	Mean Dose < 34Gy	32.52Gy	32.35Gy
Heart	V60Gy < 33%	8.60%	8.71%
	V45Gy < 66%	17.53%	19.16%
	V40Gy < 100%	19.98%	23.16%

Appendix C

Table 1

Normal tissue complication probabilities for grade 2+ radiation pneumonitis are presented for NTCP models that account for both dose to functional sub-volumes and dose to the total lung.

Grade 2+ Toxicity			
Dose Metrics for NTCP Model	**Mean Toxicity Probability – Clinical Plan**	**Mean Toxicity Probability – Functional Plan**	**Absolute Reduction**
fV5Gy + V5Gy	44.9%	35.8%	9.1%
fV10Gy + V10Gy	42.2%	31.8%	10.4%
fV20Gy + V20Gy	39.9%	33.4%	6.5%
fV30Gy + V30Gy	39.7%	33.2%	6.4%
fMLD + MLD	34.8%	34.1%	0.6%

Table 2

Normal tissue complication probabilities for grade 3+ radiation pneumonitis are presented for NTCP models that account for both dose to functional sub-volumes and dose to the total lung.

Grade 3+ Toxicity			
Dose Metrics for NTCP Model	**Mean Toxicity Probability – Clinical Plan**	**Mean Toxicity Probability – Functional Plan**	**Absolute Reduction**
fV5Gy + V5Gy	23.2%	19.0%	4.2%
fV10Gy + V10Gy	22.2%	17.5%	4.7%
fV20Gy + V20Gy	20.2%	16.6%	3.7%
fV30Gy + V30Gy	20.1%	15.9%	4.2%
fMLD + MLD	17.7%	17.7%	0.0%

References

1. Society AC. Cancer facts & figures 2016. American Cancer Society; 2016.
2. Yaremko BP, Guerrero TM, Noyola-Martinez J, et al. Reduction of normal lung irradiation in locally advanced non-small-cell lung cancer patients, using ventilation images for functional avoidance. International Journal of Radiation Oncology Biology Physics. 2007; 68:562–571.

Author Manuscript Author Manuscript Author Manuscript Author Manuscript

3. Martel MK, Ten Haken RK, Hazuka MB, et al. Estimation of tumor control probability model parameters from 3-d dose distributions of non-small cell lung cancer patients. Lung Cancer. 1999; 24:31–37. [PubMed: 10403692]
4. Graham MV, Purdy JA, Emami B, et al. Clinical dose-volume histogram analysis for pneumonitis after 3d treatment for non-small cell lung cancer (nsclc). International Journal of Radiation Oncology Biology Physics. 1999; 45:323–329.
5. Kwa SLS, Lebesque JV, Theuws JCM, et al. Radiation pneumonitis as a function of mean lung dose: An analysis of pooled data of 540 patients. International Journal of Radiation Oncology* Biology* Physics. 1998; 42:1–9.
6. Videtic GM, Hu C, Singh AK, et al. A randomized phase 2 study comparing 2 stereotactic body radiation therapy schedules for medically inoperable patients with stage i peripheral non-small cell lung cancer: Nrg oncology rtog 0915 (ncctg n0927). Int J Radiat Oncol Biol Phys. 2015; 93:757–64. [PubMed: 26530743]
7. Bradley JD, Paulus R, Komaki R, et al. A randomized phase iii comparison of standard-dose (60 gy) versus high-dose (74 gy) conformal chemoradiotherapy with or without cetuximab for stage iii non-small cell lung cancer: Results on radiation dose in rtog 0617. J Clin Oncol. 2013; 31:7501.
8. Bradley J, Graham MV, Winter K, et al. Toxicity and outcome results of rtog 9311: A phase i-ii dose- escalation study using three-dimensional conformal radiotherapy in patients with inoperable non-small-cell lung carcinoma. International Journal of Radioation Oncology*Biology*Physics. 2005; 61:318–328.
9. Vinogradskiy Y, Gan G, Castillo R, et al. Quantitative assessment of lung function in stage i and stage iii lung radiation therapy patients using 4dct-based ventilation imaging. International Journal of Radiation Oncology Biology Physics. 2012; 84:S754–S754.
11. Yamamoto T, Kabus S, Bal M, et al. The first patient treatment of computed tomography ventilation functional image-guided radiotherapy for lung cancer. Radiotherapy and Oncology. 2015
12. Yamamoto T, Kabus S, von Berg J, et al. Impact of four-dimensional computed tomography pulmonary ventilation imaging-based functional avoidance for lung cancer radiotherapy. International Journal of Radiation Oncology Biology Physics. 2011; 79:279–288.
13. Yamamoto T, Kabus S, von Berg J, et al. Impact of four-dimensional ct-derived pulmonary ventilation images on radiotherapy treatment planning for lung cancer. International Journal of Radiation Oncology Biology Physics. 2009; 75:S443–S443.
14. Lavrenkov K, Christian JA, Partridge M, et al. A potential to reduce pulmonary toxicity: The use of perfusion spect with imrt for functional lung avoidance in radiotherapy of non-small cell lung cancer. Radiother Oncol. 2007; 83:156–62. [PubMed: 17493699]
15. Bates EL, Bragg CM, Wild JM, et al. Functional image-based radiotherapy planning for non-small cell lung cancer: A simulation study. Radiother Oncol. 2009; 93:32–6. [PubMed: 19552978]
16. Hodge CW, Tomé WA, Fain SB, et al. On the use of hyperpolarized helium mri for conformal avoidance lung radiotherapy. Med Dosim. 2010; 35:297–303. [PubMed: 19944585]
17. Kabus S, von Berg J, Yamamoto T, et al. Lung ventilation estimation based on 4d-ct imaging. :73–83.
18. Guerrero T, Sanders K, Castillo E, et al. Dynamic ventilation imaging from four-dimensional computed tomography. Phys Med Biol. 2006; 51:777–91. [PubMed: 16467578]
19. Reinhardt JM, Ding K, Cao K, et al. Registration-based estimates of local lung tissue expansion compared to xenon ct measures of specific ventilation. Medical Image Analysis. 2008; 12:752–763. [PubMed: 18501665]
20. Christensen GE, Song JH, Lu W, et al. Tracking lung tissue motion and expansion/compression with inverse consistent image registration and spirometry. Medical physics. 2007; 34:2155–2163. [PubMed: 17654918]
22. Du KF, Bayouth JE, Cao KL, et al. Reproducibility of registration-based measures of lung tissue expansion. Medical Physics. 2012; 39:1595–1608. [PubMed: 22380392]
23. Yamamoto T, Kabus S, Lorenz C, et al. Pulmonary ventilation imaging based on 4-dimensional computed tomography: Comparison with pulmonary function tests and spect ventilation images. International Journal of Radiation Oncology* Biology* Physics. 2014

Author Manuscript Author Manuscript Author Manuscript Author Manuscript

24. Brennan D, Schubert L, Diot Q, et al. Clinical validation of 4-dimensional computed tomography ventilation with pulmonary function test data. International Journal of Radiation Oncology Biology Physics. 2015; 92:423–429.
25. Fuld MK, Easley RB, Saba OI, et al. Ct-measured regional specific volume change reflects regional ventilation in supine sheep. Journal of Applied Physiology. 2008; 104:1177–1184. [PubMed: 18258804]
26. Mathew L, Wheatley A, Castillo R, et al. Hyperpolarized he-3 magnetic resonance imaging: Comparison with four-dimensional x-ray computed tomography imaging in lung cancer. Academic Radiology. 2012; 19:1546–1553. [PubMed: 22999648]
27. Vinogradskiy Y, Koo PJ, Castillo R, et al. Comparison of 4-dimensional computed tomography ventilation with nuclear medicine ventilation-perfusion imaging: A clinical validation study. International Journal of Radiation Oncology Biology Physics. 2014; 89:199–205.
28. Kipritidis J, Siva S, Hofman MS, et al. Validating and improving ct ventilation imaging by correlating with ventilation 4d-pet/ct using 68ga-labeled nanoparticles. Medical physics. 2014; 41:011910. [PubMed: 24387518]
29. Vinogradskiy Y, Castillo R, Castillo E, et al. Use of 4-dimensional computed tomography-based ventilation imaging to correlate lung dose and function with clinical outcomes. International Journal of Radiation Oncology Biology Physics. 2013; 86:366–371.
30. Yamamoto T, Kabus S, Klinder T, et al. Investigation of four-dimensional computed tomography-based pulmonary ventilation imaging in patients with emphysematous lung regions. Physics in Medicine and Biology. 2011; 56:2279–2298. [PubMed: 21411868]
31. Bayouth J, Du K, Christensen G, et al. Establishing a relationship between radiosensitivity of lung tissue and ventilation. International Journal of Radiation Oncology* Biology* Physics. 2012; 84:S31–S32.
32. Ding K, Bayouth JE, Buatti JM, et al. 4dct-based measurement of changes in pulmonary function following a course of radiation therapy. Medical Physics. 2010; 37:1261–1272. [PubMed: 20384264]
33. Castillo E, Castillo R, Martinez J, et al. Four-dimensional deformable image registration using trajectory modeling. Physics in Medicine and Biology. 2010; 55:305–327. [PubMed: 20009196]
34. Simon BA. Non-invasive imaging of regional lung function using x-ray computed tomography. Journal of Clinical Monitoring and Computing. 2000; 16:433–442. [PubMed: 12580227]
35. Efron, B., Tibshirani, RJ. An introduction to the bootstrap. new york NY: Chapman and Hall; 1993.
36. Lind PA, Marks LB, Hollis D, et al. Receiver operating characteristic curves to assess predictors of radiation-induced symptomatic lung injury. International Journal of Radiation Oncology Biology Physics. 2002; 54:340–347.
37. Lan F, Jeudy J, Senan S, et al. Should regional ventilation function be considered during radiation treatment planning to prevent radiation-induced complications? Medical Physics. 2016; 43:5072. [PubMed: 27587037]
38. Seppenwoolde Y, Engelsman M, De Jaeger K, et al. Optimizing radiation treatment plans for lung cancer using lung perfusion information. Radiotherapy and oncology. 2002; 63:165–177. [PubMed: 12063006]
39. Munawar I, Yaremko BP, Craig J, et al. Intensity modulated radiotherapy of non-small-cell lung cancer incorporating spect ventilation imaging. Medical Physics. 2010; 37:1863–1872. [PubMed: 20443508]
40. Christian JA, Partridge M, Nioutsikou E, et al. The incorporation of spect functional lung imaging into inverse radiotherapy planning for non-small cell lung cancer. Radiotherapy and oncology. 2005; 77:271–277. [PubMed: 16274762]
41. Siva S, Thomas R, Callahan J, et al. High-resolution pulmonary ventilation and perfusion pet/ct allows for functionally adapted intensity modulated radiotherapy in lung cancer. Radiotherapy and Oncology. 2015
42. Kida S, Bal M, Kabus S, et al. Ct ventilation functional image-based imrt treatment plans are comparable to spect ventilation functional image-based plans. Radiotherapy and Oncology. 2016; 118:521–527. [PubMed: 26922488]

Author Manuscript Author Manuscript Author Manuscript Author Manuscript

43. Yamamoto T, Kabus S, Lorenz C, et al. 4d ct lung ventilation images are affected by the 4d ct sorting method. Medical Physics. 2013; 40

44. Du K, Reinhardt JM, Christensen GE, et al. Respiratory effort correction strategies to improve the reproducibility of lung expansion measurements. Medical physics. 2013; 40:123504. [PubMed: 24320544]

45. Vinogradskiy YY, Castillo R, Castillo E, et al. Use of weekly 4dct-based ventilation maps to quantify changes in lung function for patients undergoing radiation therapy. Medical Physics. 2012; 39:289–298. [PubMed: 22225299]

47. Shioyama Y, Jang SY, Liu HH, et al. Preserving functional lung using perfusion imaging and intensity-modulated radiation therapy for advanced-stage non–small cell lung cancer. International Journal of Radiation Oncology* Biology* Physics. 2007; 68:1349–1358.

48. Seppenwoolde Y, Muller SH, Theuws J, et al. Radiation dose-effect relations and local recovery in perfusion for patients with non–small-cell lung cancer. International Journal of Radiation Oncology* Biology* Physics. 2000; 47:681–690.

Author Manuscript Author Manuscript Author Manuscript Author Manuscript

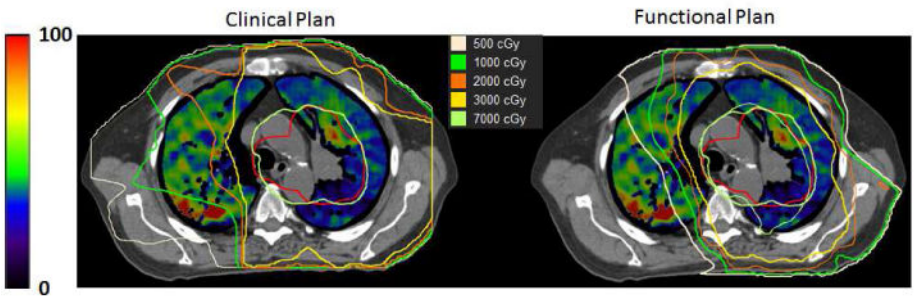

Figure 1.

A representative example comparing a clinical plan (left) to a functional avoidance plan (right) is presented. A CT ventilation image shows regional functionality (scale on the left) with the PTV contoured in red and isodose lines overlaid on the images.

Author Manuscript Author Manuscript Author Manuscript Author Manuscript

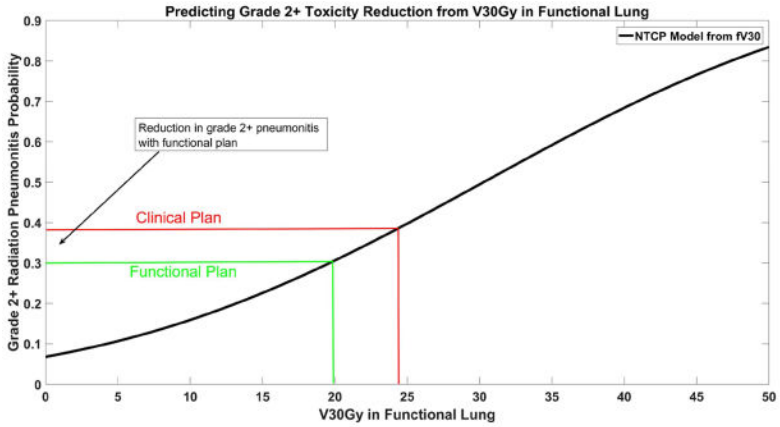

Figure 2.

The NTCP model for grade 2+ radiation pneumonitis is shown as a function of the volume of functional lung receiving 30Gy (fV30Gy). Toxicity probabilities are calculated using the mean fV30Gy in the clinical and functional plans.

Author Manuscript Author Manuscript Author Manuscript Author Manuscript

Table 1

Results of the maximum-likelihood modeling of normal tissue complication probabilities as a function of functional lung volume metrics (fVXGy) and total lung volume metrics (VXGy). Values in parentheses represent the 95% confidence interval of the fitting parameters.

	Grade 2+ Pneumonitis				Grade 3+ Pneumonitis			
Dose Metric	**p-Value**	**AUC**	**m**	**TD50**	**p-Value**	**AUC**	**m**	**TD50**
fV5Gy	<0.01	0.693	0.479 (0.185-0.773)	72.7 (5.1-140.3)	0.82	0.537	1.020 (-0.304-2.343)	427.1 (-3323.0-4177.2)
V5Gy	0.05	0.637	0.577 (0.100-1.054)	77.9 (-22.5-178.2)	0.68	0.506	1.889 (-3.427-7.205)	-105.3 (-679.1-468.5)
fV10Gy	<0.01	0.718	0.530 (0.210-0.850)	54.1 (4.1-104.0)	0.27	0.574	0.689 (0.143-1.235)	106.4 (-101.0-313.8)
V10Gy	0.13	0.614	0.757 (-0.003-1.517)	63.8 (-40.9-168.6)	0.85	0.537	1.409 (-1.388-4.207)	-254.3 (-2939.6-2431.1)
fV20Gy	<0.01	0.707	0.548 (0.254-0.841)	35.9 (6.7-65.1)	0.01	0.674	0.473 (0.232-0.714)	50.8 (3.8-97.7)
V20Gy	0.36	0.545	1.095 (-0.464-2.653)	52.7 (-83.3-188.7)	0.49	0.519	0.742 (-0.072-1.557)	90.5 (-184.2-365.2)
fV30Gy	<0.01	0.682	0.670 (0.286-1.054)	30.3 (3.4-57.2)	0.01	0.671	0.517 (0.260-0.775)	43.6 (2.9-84.3)
V30Gy	0.75	0.508	1.934 (-2.613-6.480)	76.0 (-430.0-582.1)	0.53	0.519	0.787 (-0.080-1.654)	83.1 (-194.2-360.4)
fMLD	<0.01	0.723	0.672 (0.440-0.904)	30.3 (13.3-47.4)	0.02	0.648	0.519 (0.268-0.770)	43.7 (13.3-74.2)
MLD	0.12	0.584	0.672 (0.003-1.41)	26.3 (-15.6-68.1)	0.29	0.545	0.586 (0.017-1.155)	40.8 (-44.6-126.1)

Int J Radiat Oncol Biol Phys. Author manuscript; available in PMC 2018 October 01.

Author Manuscript

Author Manuscript

Author Manuscript

Author Manuscript

Table 2

The percentage volume of the functional lung receiving ≥5Gy, 10Gy, 20Gy, and 30Gy for clinical and functional plans are presented along with the mean dose to functional lung.

Dose Metric Parameter	Mean Dose Metric - Clinical Plan	Mean Dose Metric - Functional Plan
fV5Gy (%)	64.8	60.8
fV10Gy (%)	47.0	40.8
fV20Gy (%)	30.1	26.8
fV30Gy (%)	24.2	19.9
fMLD (Gy)	19.0	17.8

Author Manuscript

Author Manuscript

Author Manuscript

Author Manuscript

Table 3

Normal tissue complication probabilities for grade 2+ radiation pneumonitis are presented for the average functional lung volume metrics for the clinical plans and functional avoidance plans. In parentheses is the 95% confidence intervals in the NTCP values and toxicity reduction as determined during bootstrap analysis. The range of toxicity reductions among the 30 patients re-planned with functional avoidance techniques is also presented. Positive numbers correspond to a decreased risk in toxicity while negative numbers correspond to an increased risk of toxicity.

Grade 2+ Toxicity				
Dose Metric for NTCP Model	**Toxicity Probability of the Mean – Clinical Plan**	**Toxicity Probability of the Mean – Functional Plan**	**Absolute Reduction**	**Range of Reductions**
fV5Gy	41.0% (28.2%-53.8%)	36.6% (24.1%-48.8%)	4.4% (1.3% - 8.1%)	-30.1% - 40.5%
fV10Gy	40.2% (27.8% -54.3%)	32.2% (20.3%-44.3%)	8.0% (2.8% - 16.0%)	-25.3% - 52.3%
fV20Gy	38.4% (26.2%-51.8%)	32.2% (20.3%-44.9%)	6.3% (2.9% - 10.1%)	-16.9% - 19.4%
fV30Gy	38.3% (26.4%-51.7%)	30.5% (18.9%-42.8%)	7.8% (3.2% - 13.5%)	-8.3% - 18.9%
fMLD	39.6% (27.2%-53.5%)	34.8% (22.4%-47.8%)	4.8% (2.3% - 7.9%)	-30.3% - 25.6%

Author Manuscript

Author Manuscript

Author Manuscript

Author Manuscript

Table 4

Normal tissue complication probabilities for grade 3+ radiation pneumonitis are presented for the average functional lung volume metrics for the clinical plans and functional avoidance plans. In parentheses is the 95% confidence intervals in the NTCP values and toxicity reduction as determined during bootstrap analysis. The range of toxicity reductions among the 30 patients re-planned with functional avoidance techniques is also presented. Positive numbers correspond to a decreased risk in toxicity while negative numbers correspond to an increased risk of toxicity.

Grade 3+ Toxicity				
Dose Metric for NTCP Model	**Toxicity Probability of the Mean – Clinical Plan**	**Toxicity Probability of the Mean – Functional Plan**	**Absolute Reduction**	**Range of Reductions**
fV20Gy	19.5% (9.3%-29.5%)	15.9% (6.3%-25.2%)	3.6% (0.8% - 6.1%)	-15.4% - 14.3%
fV30Gy	19.6% (9.1%-29.4%)	14.7% (5.4%-24.0%)	4.8% (0.8% - 8.4%)	-7.0% - 14.7%
fMLD	20.3% (10.0%-30.4%)	17.9% (7.9%-27.3%)	2.4% (0.2% - 4.3%)	-24.4% - 16.4%